Table S1. Arg accessibility to solvents in the 3D models of PAD3 [#].

% of accessibility to solvents												
PAD3 "empty" (WD8)							PAD3 "full" (WDA)					
39 Arg		20 Cit		39 Cit			39 Arg		10 Cit		39 Cit	
Position	%	Position	%	Position	%		Position	%	Position	%	Position	%
Arg-5	30	Arg-5	<30	Cit-5	<30		Arg-5	<30	Arg-5	<30	Cit-5	<30
Arg-8	50	Cit-8	30	Cit-8	30		Arg-8	30	Arg-8	<30	Cit-8	40
Arg-58	50	Cit-58	50	Cit-58	50		Arg-58	40	Cit-58	50	Cit-58	50
Arg-60	50	Cit-60	30	Cit-60	50		Arg-60	50	Cit-60	50	Cit-60	50
Arg-62	40	Cit-62	30	Cit-62	40		Arg-62	50	Cit-62	40	Cit-62	40
Arg-66	50	Cit-66	40	Cit-66	50		Arg-66	<30	Arg-66	<30	Cit-66	<30
Arg-67	<30	Arg-67	30	Cit-67	30		Arg-67	30	Arg-67	40	Cit-67	50
Arg-69	<30	Arg-69	<30	Cit-69	30		Arg-69	<30	Arg-69	<30	Cit-69	30
Arg-128	50	Cit-128	40	Cit-128	30		Arg-128	40	Cit-128	40	Cit-128	40
Arg-131	40	Cit-131	<30	Cit-131	<30		Arg-131	50	Cit-131	60	Cit-131	70
Arg-137	40	Cit-137	30	Cit-137	50		Arg-137	<30	Arg-137	<30	Cit-137	30
Arg-156	30	Arg-156	<30	Cit-156	<30		Arg-156	<30	Arg-156	<30	Cit-156	<30
Arg-186	<30	Arg-186	<30	Cit-186	<30		Arg-186	<30	Arg-186	<30	Cit-186	<30
Arg-210	<30	Arg-210	<30	Cit-210	<30		Arg-210	<30	Arg-210	<30	Cit-210	<30
Arg-227	50	Cit-227	40	Cit-227	<30		Arg-227	<30	Arg-227	<30	Cit-227	<30
Arg-241	<30	Arg-241	<30	Cit-241	<30		Arg-241	<30	Arg-241	<30	Cit-241	<30
Arg-248	30	Arg-248	30	Cit-248	<30		Arg-248	<30	Arg-248	<30	Cit-248	<30
Arg-292	<30	Arg-292	<30	Cit-292	<30		Arg-292	<30	Arg-292	<30	Cit-292	<30
Arg-312	40	Cit-312	30	Cit-312	50		Arg-312	<30	Arg-312	<30	Cit-312	<30
Arg-314	50	Cit-314	60	Cit-314	50		Arg-314	<30	Arg-314	<30	Cit-314	<30
Arg-328	40	Cit-328	40	Cit-328	50		Arg-328	40	Cit-328	50	Cit-328	50
Arg-343	60	Cit-343	60	Cit-343	60		Arg-343	30	Arg-343	30	Cit-343	30
Arg-346	50	Cit-346	30	Cit-346	40		Arg-346	<30	Arg-346	<30	Cit-346	<30
Arg-372	40	Cit-372	30	Cit-372	40		Arg-372	<30	Arg-372	<30	Cit-372	<30
Arg-383	60	Cit-383	60	Cit-383	60		Arg-383	30	Arg-383	<30	Cit-383	40
Arg-394	<30	Arg-394	<30	Cit-394	<30		Arg-394	<30	Arg-394	<30	Cit-394	<30
Arg-397	30	Arg-397	40	Cit-397	40		Arg-397	30	Arg-397	40	Cit-397	40
Arg-399	50	Cit-399	50	Cit-399	60		Arg-399	40	Cit-399	40	Cit-399	40
Arg-427	<30	Arg-427	<30	Cit-427	<30		Arg-427	<30	Arg-427	<30	Cit-427	<30
Arg-440	<30	Arg-440	<30	Cit-440	<30		Arg-440	<30	Arg-440	<30	Cit-440	<30
Arg-441	<30	Arg-441	<30	Cit-441	<30		Arg-441	<30	Arg-441	<30	Cit-441	<30
Arg-447	<30	Arg-447	<30	Cit-447	<30		Arg-447	<30	Arg-447	<30	Cit-447	<30
Arg-487	<30	Arg-487	<30	Cit-487	<30		Arg-487	<30	Arg-487	<30	Cit-487	<30
Arg-510	60	Cit-510	50	Cit-510	50		Arg-510	60	Cit-510	40	Cit-510	50
Arg-552	<30	Arg-552	<30	Cit-552	<30		Arg-552	<30	Arg-552	<30	Cit-552	<30
Arg-557	40	Cit-557	40	Cit-557	50		Arg-557	40	Cit-557	40	Cit-557	40
Arg-577	40	Cit-577	50	Cit-577	40		Arg-577	50	Cit-577	30	Cit-577	30
Arg-618	30	Arg-618	30	Cit-618	30		Arg-618	<30	Arg-618	<30	Cit-618	<30
Arg-652	<30	Arg-652	<30	Cit-652	<30		Arg-652	<30	Arg-652	<30	Cit-652	<30

[#] Three-dimensional models of PAD3 without bound-calcium and substrate (empty) or with bound-calcium and -benzoyl-L-arginine amide (full) were deduced from the PAD4 structures and the amino-acid sequence of PAD3. For each Arg, the accessibility to the solvents (in %) was computed. The most accessible Arg (% of accessibility ≥ 40) were then replaced by Cit, and the accessibility computed again. The same was done with all Arg replaced by Cit.

Table S2. Volumes and surface areas of the entire molecule or C-terminal domain of PAD3 [#].

3D models of PAD3	Volume	Surface
Entire PAD3		
PAD3 "empty" WD8 39 Arg	90669	31154
PAD3 "empty" WD8 20 Cit	90905	29681
PAD3 "full" WDA 39 Arg	91547	25107
PAD3 "full" WDA 10 Cit	90976	24966
C-terminal domain of PAD3		
C-ter PAD3 "empty" WD8 39 Arg	50871	17172
C-ter PAD3 "empty" WD8 20 Cit	50704	16639
C-ter PAD3 "full" WDA 39 Arg	51572	13116
C-ter PAD3 "full" WDA 10 Cit	50834	12861

[#] Volumes ($Å^3$) and surface areas ($Å^2$) were computed for PAD3 three-dimensional structures either without bound-calcium and substrate (empty) or with bound-calcium and -benzoyl-L-arginine amide as a substrate (full) using "Swiss-Pdb Viewer Deep View 4.0.1". The same evaluation was made after substitutions of the most accessible Arg to Cit. The same was done for the C-terminal (C-ter) domain of PAD3 (from Pro-295 to Pro-664) containing the active site.

Figure S1: Schematic representation of the formula to evaluate a tetrahedron volume.

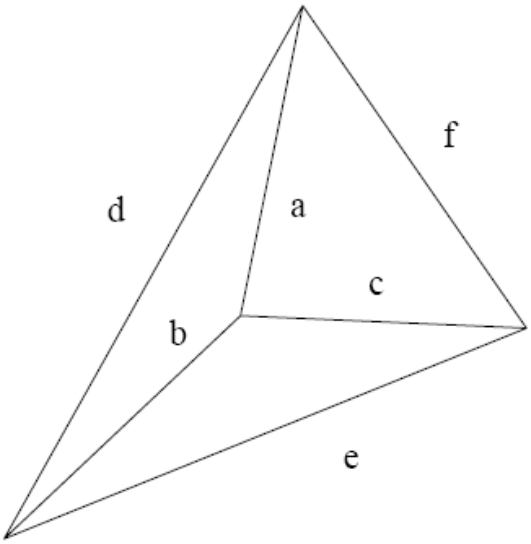

$$V = 1/12 \sqrt{(P - Q + R)}$$

$$P = 4\, a^2\, b^2\, c^2$$

$$Q = a^2.E^2 - b^2.F^2 - c^2.D^2$$

$$R = D.\, E.\, F$$

$$D = a^2 + b^2 - d^2$$

$$E = b^2 + c^2 - e^2$$

$$F = a^2 + c^2 - f^2$$

Figure S2: Topological 3D models of PAD3 [#].

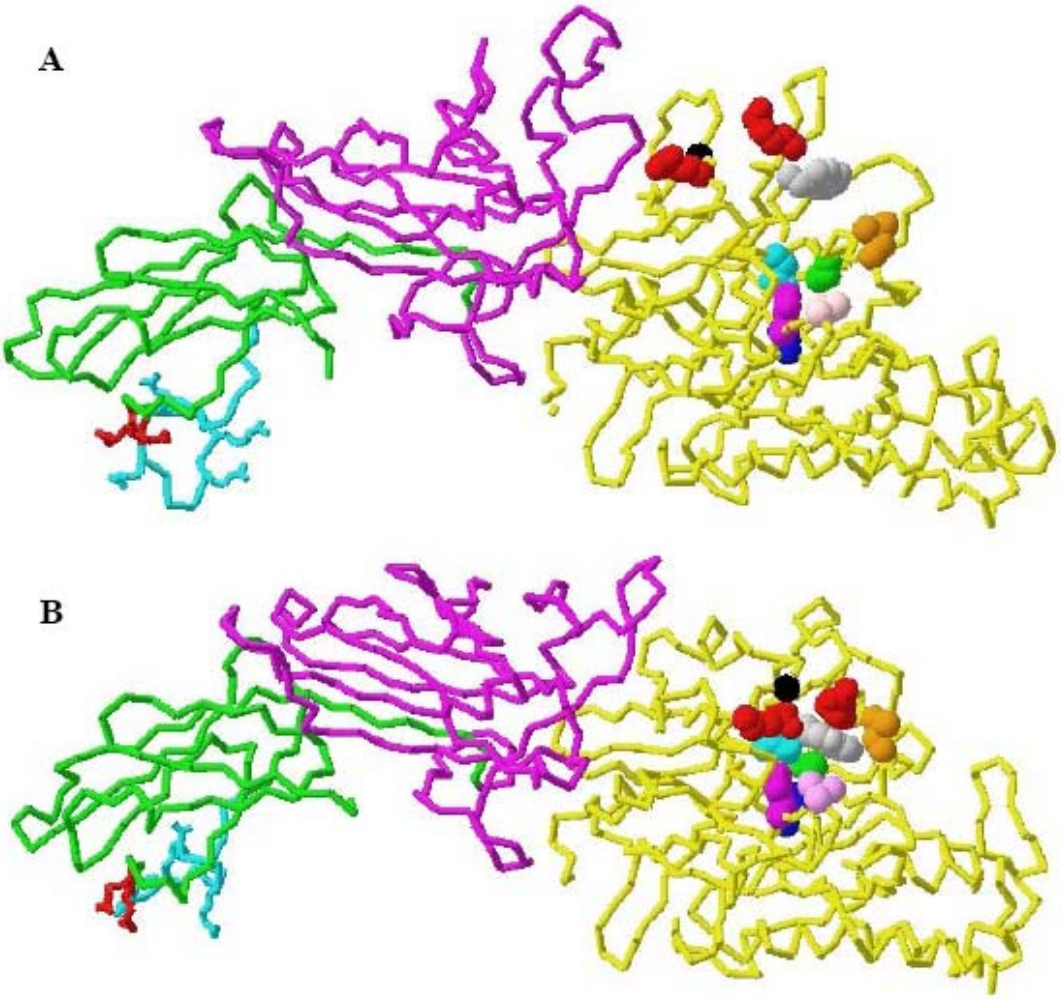

[#] 3D modeling of **A**, Ca^{2+}-free PAD3 (derived from 1WD8) and **B,** Ca^{2+}-bound PAD3. The immunoglobulin-like sub-domains 1 (residues 1-123) and 2 (residues 124-294) are in green and purple respectively, and the C-terminal domain (295-664) is in yellow. The lateral chains of the arginines of the peptide 49-66 in sky blue and of the Arg-67 and Arg-69 in red are reported on the structure to show their accessibility. Ten amino-acids major in the active site are shown using space-filling representation. The arginine (Arg-372), glycine (Gly-374) and leucine (Leu-640), probably involved in the substrate specificity of PAD3 are in red, black and orange respectively. The arginine (Arg-346), tryptophan (Trp-347) and valine (Val-468) recently reported as important in the active site of PAD4 and conserved in the other PADs are in red, grey and pink. Among the four amino-acids directly involved in the deimination reaction, the two aspartic acids (Asp-350 and Asp-472) are in sky

blue and blue navy, respectively, the histidine (His-470) is in purple and the cysteine (Cys-646) in green. As observed for PAD1 and PAD4 [1], the two structures are roughly superimposable.

Figure S3: No decrease in the expression of Pad1 and Pad3 in the epidermis of VDR-null as compared to wild type mice [#].

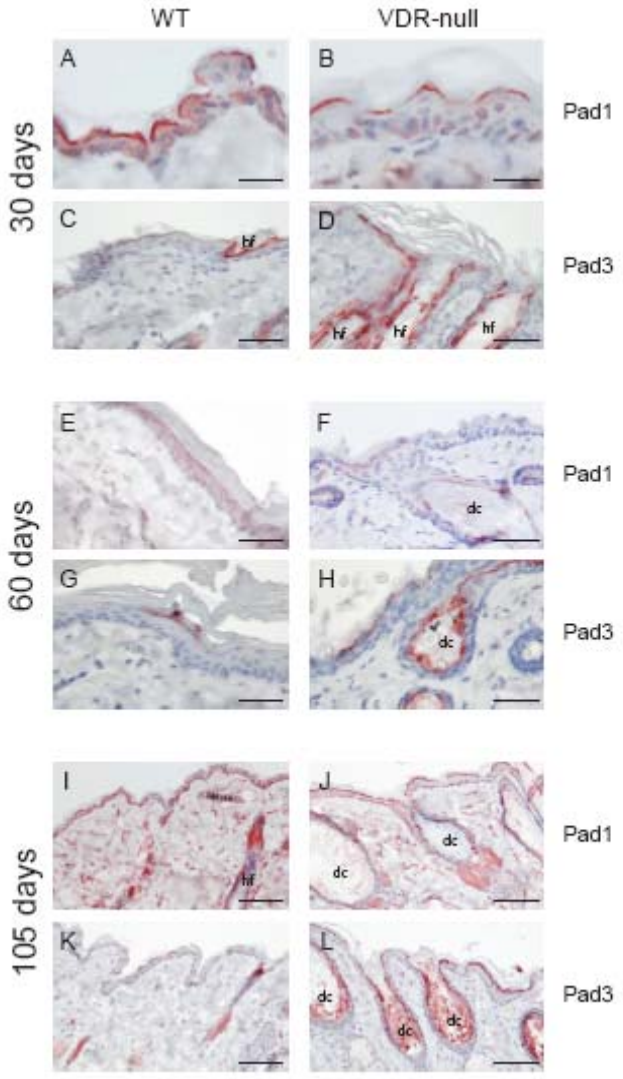

[#] Paraffin-embedded sections of 30 (A-D), 60 (E-H) and 105 (I-L) days old wild type (WT) (A, C, E, G, I and K) and VDR-null mice (B, D, F, H, J and L) were analyzed by immunohistochemical staining with the purified polyclonal antibodies against Pad1 and Pad3. Pad1 and Pad3 are located preferentially in the *stratum granulosum* of both WT and VDR-null mouse epidermis. No decrease in the detection level of both Pad1 and Pad3 was evidenced in the VDR-null mouse epidermis. Moreover Pad3 but not Pad1 was located in dermal cysts of the VDR-null mouse skin (H and L).
hf (hair follicle); dc (dermal cyst). Bars in A -D = 100 μm; bar in E-L = 200 μm.

Method: Paraffin-embedded skin sections of WT and VDR-null mice were a kind gift from H. Palmer and G. Carmeliet (Cancer Research UK Cambridge research Institute, Cambridge,UK). Skin sections were deparaffinised and rehydrated using standard procedures. Immunohistochemistry was performed using the Histostain-Plus kit (Zymed) according to the manufacturer's instructions. Pad1 and Pad3 were detected using already described and validated isotype specific rabbit antipeptide antibodies at a concentration of 1 and 0.3 μg/ml respectively. Before applying the primary antibodies, tissue sections were processed for heat-induced epitope retrieval using a target retrieval solution at pH 9.9 (Dako, #S3308) and pH 9 (Dako, #S2368) for Pad1 and Pad3 detection respectively. The slides were then incubated in a humidified chamber with their corresponding primary antibodies overnight at 4°C. Colour was developed in an aminoethyl carbazole substrate solution and the tissues were counterstained with hematoxylin. A normal rabbit antiserum was used as a negative control.